



# Frequency dependent fluid damping of micro/nano flexural resonators: Experiment, model and analysis

Weibin Zhang\*, Kimberly Turner

*Mechanical Engineering, University of California at Santa Barbara, Santa Barbara, CA 93106-5070, United States*

Received 19 March 2006; accepted 4 June 2006

## Abstract

This research systematically investigates the fluid damping for micromachined beam-type resonators with high resonant frequencies. The work is aimed to find a general fluid damping law which can quantitatively be used as a design tool for the resonance-based micro sensors by accurately predicting the quality factor for resonators operated in air or liquid. Micro-cantilevers with different dimensions are fabricated and tested in order to extract the damping characteristics. Combined with dimensional analysis, a novel linear fluid damping model is proposed, considering the effects from both device's dimension and the resonant frequency. Further by numerical analysis, the model is generalized to resonators with differently shaped cross-sections. Also the proposed fluid damping model provides an attractive way to use simple beam-type resonators as fluid viscosity sensors and air pressure sensors.

© 2006 Elsevier B.V. All rights reserved.

**Keywords:** Resonator; Quality factor; Fluid damping; Drag force

## 1. Introduction

Micromachined beam-type resonant structures are widely applied as high-performance sensors [1,2]. One of the most important parameters for the resonators is the mechanical quality factor ( $Q$ ). In general, for a resonator, sensing can be based on a change of resonant frequency, amplitude or phase. High  $Q$  factor will result in a sharp frequency response in these resonant parameters, which leads to high sensitivity [3]. Understanding the factors that dominate the damping of the resonators and thereby determining  $Q$  are extremely important. It not only helps to improve  $Q$  factor prediction, but also helps to optimize sensor design.

Most micro/nano scale resonators require vacuum operating condition to achieve high  $Q$  factor. There are also many useful applications involve sensing in real-world environments, such as air or liquid [4,5]. Quality factor in flexural beam is impacted negatively by fluid damping. An open design problem in micro/nano-sensors is maximizing sensitivity in environments of increased fluid damping. For example, in [5], the authors

demonstrate a parametric resonance based mass sensor which shows good sensitivity when operated in air. In this work, we focus our interest on the fluid damping defined by cases where the fluid drag force is the dominant damping source. We assume that the resonator is isolated from other objects, so the effects of such as anchors and squeeze-film damping are not considered. For a beam-type resonator, we detail in this work that there are three important factors which influence  $Q$  factor: dimensions, resonant frequency and cross-sectional shape.

High resonant frequency is a key advantage of micro/nano resonators for certain applications [6]. For “in-fluid” oscillation in this region, the fluid damping characteristics behave dramatically different compared to the low frequency or the steady flow cases, which results in frequency-dependent fluid damping. On the other hand, the resonator dimensions, especially those whose directions are perpendicular to the flow, play an important role in the fluid damping. The cross-sectional shape is relatively less controllable from design point of view, due to the limitations of micro machining methods. Resonators with three kinds of cross-section shapes are considered in detail: cantilever with rectangular cross-section, carbon nanotube with circular cross-section, and scanning probe with trapezoid cross-section.

There has been little research done to quantitatively explore this frequency-dependent damping in a high damping medium.

\* Corresponding author. Tel.: +1 805 893 7849; fax: +1 805 893 8651.  
E-mail address: [weibin@engr.ucsb.edu](mailto:weibin@engr.ucsb.edu) (W. Zhang).

### Nomenclature

$(a, b)$	dimensionless coefficients in (10)
$C_{\text{damping}} = (F/u)$	damping coefficient (N s/m <sup>2</sup> )
$d_1, d_2$	dimensions of the elliptic or rectangular cross-section (Fig. 7), $d_1 \parallel u$ , $d_2 \perp u$
$F$	fluid drag force per unit length (N/m)
$Re$	Reynolds number
$u$	velocity of the resonator (m/s)

### Greek letters

$\delta$	penetration depth defined in (4) (m)
$\gamma$	Euler's constant ( $\approx 0.577$ )
$\lambda$	dimensionless parameter defined in (5)
$\mu$	viscosity of the fluid (kg/m s)
$\rho$	density of the fluid (kg/m <sup>3</sup> )
$\omega$	resonant angular frequency

For air damping, Newell presented a widely-used formula of Q-factor for an oscillatory cantilever with rectangular cross-section [7], from which the fluid damping coefficient can be expressed as:

$$C_{\text{damping}} \simeq 24\mu \quad (1)$$

where  $F$  is the fluid drag force per unit length on the cantilever,  $\mu$  is the fluid viscosity and  $u$  is the velocity of the cantilever. The drag force shown in (1) is independent of resonant frequency and device dimensions (such as width and thickness). While investigating the pressure dependent damping of a cantilever, Blom [8] observed the pressure and resonant frequency effects on air damping. The effects are explained using the drag force of an oscillatory sphere [9].

In this paper, motivated by the experimental observations from MEMS cantilevers, a new linear fluid damping model is proposed for the beam-type resonators. Using numerical analysis, the model is generalized to other resonators with differently shaped cross-sections. Finally a general fluid damping law is achieved with limited overall error. Two attractive potential applications for simple beams are discussed: fluid viscosity sensor and air pressure sensor.

## 2. Linear fluid damping model

### 2.1. Device description and experimental observations

A batch of suspended MEMS cantilevers with different dimensions are fabricated using silicon-on-insulator (SOI) wafers (Fig. 1). The length varies from 100 to 800  $\mu\text{m}$  and the width varies from 10 to 50  $\mu\text{m}$ . The thickness for all the devices is uniformly 5  $\mu\text{m}$ . The cantilevers are actuated by a piezoelectric base/anchor shaker. A laser-vibrometer setup [10] is used to capture the harmonic frequency response of the end-point displacement. From the response curve, the damping characteristics can be extracted. All the testings are carried out in ambient air ( $\mu \approx 1.870677 \times 10^{-5}$  kg/ms).

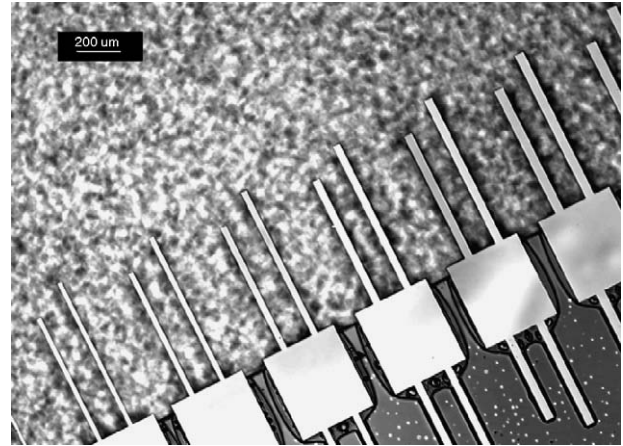


Fig. 1. Suspended silicon cantilevers with different dimensions, piezoelectrically actuated with out-of-plane motion.

For each length and each resonant mode, we test the damping coefficients ( $C_{\text{damping}}$ ) of the cantilevers with respect to different widths. It is observed that  $C_{\text{damping}}$  of the cantilevers varies with both the resonant frequency and the device's width. Typical testing results are shown in Fig. 2 (cantilevers of length 600  $\mu\text{m}$ ), which shows clearly that the damping coefficient is linearly dependent on the device width for each resonant frequency. It is also observed that this dependence varies with the resonant frequency, in other words, different resonant frequencies correspond to different slopes. The results with respect to the resonant frequency are re-plotted in Fig. 3 for different width values.

### 2.2. Linear fluid damping model

Here the fluid damping model is proposed, based on the experimental observations mentioned above together with dimensional analysis. According to classical fluid mechanics [11], the drag force of an object is proportional to the object's

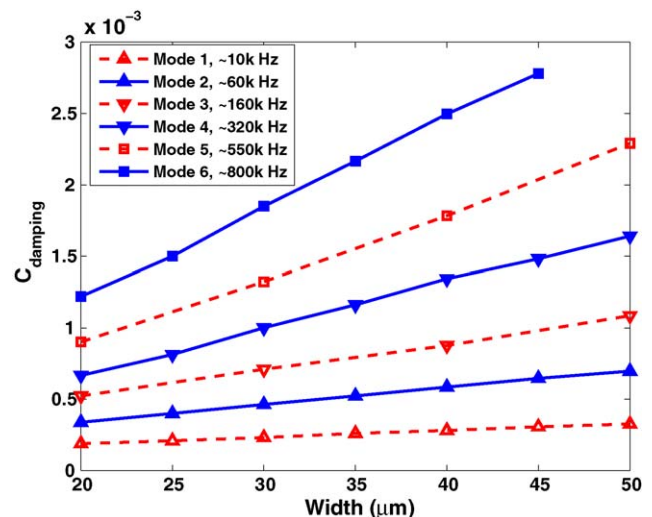


Fig. 2. Experimental results for cantilevers of length 600  $\mu\text{m}$  length, with respect to different widths.

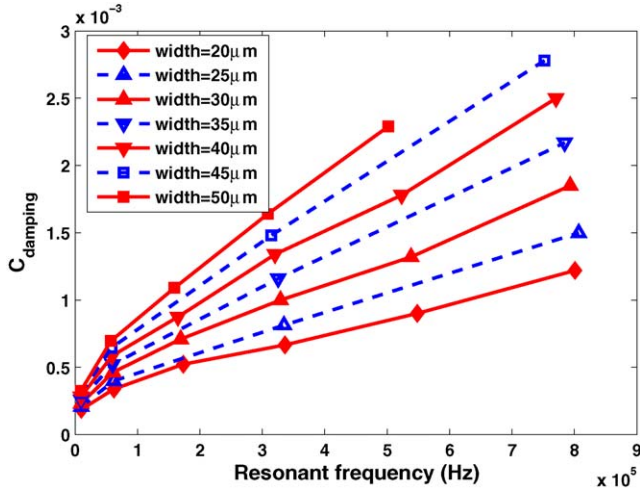


Fig. 3. Experimental results for cantilevers of length  $600 \mu\text{m}$ , with respect to different resonant frequencies.

velocity  $u$  when  $u$  is small. By referring the drag force expression of a vibrating sphere, the drag force of a vibrating cantilever has the following form:

$$F = \pi\mu u f \quad (2)$$

where  $f$  is a dimensionless function of resonant frequency ( $\omega$ ), cantilever width, fluid density ( $\rho$ ) and fluid viscosity ( $\mu$ ):

$$f = f(\text{width}, \rho, \omega, \mu) \quad (3)$$

For viscous fluid, a characteristic length  $\delta$ —called penetration depth, is usually defined [9] as:

$$\delta = \sqrt{\frac{2\mu}{\rho\omega}} \quad (4)$$

We define a dimensionless parameter  $\lambda$  as:

$$\lambda = \frac{\text{width}}{\delta} \quad (5)$$

According to the dimensional analysis in [11], function  $f$  can further be simplified:

$$f = f(\text{width}, \rho, \omega, \mu) \quad (6)$$

$$f = f(\text{width}, \delta) \quad (7)$$

$$f = f\left(\frac{\text{width}}{\delta}\right) = f(\lambda) \quad (8)$$

To be consistent with the experimental observations that  $F$  is linearly dependent on the width, as the first-order approximation, function  $f$  can be written as:

$$f = a + b\lambda \quad (9)$$

Or the corresponding damping coefficient is:

$$C_{\text{damping}} = \frac{F}{u} = \pi\mu(a + b\lambda) \quad (10)$$

where coefficient pair  $(a, b)$  is dimensionless and will be determined in detail later.

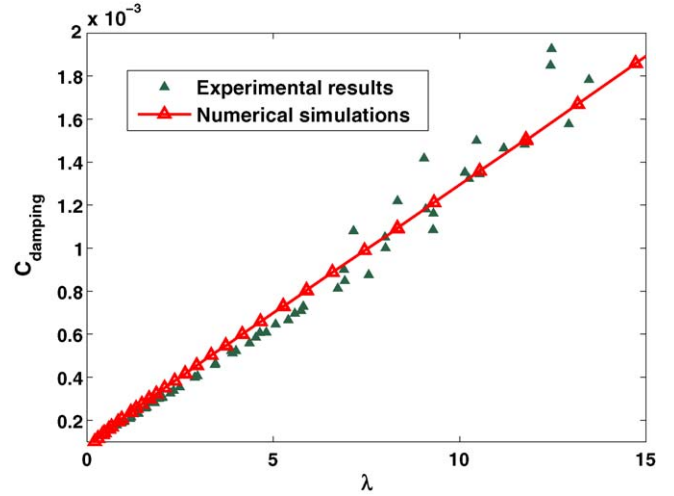


Fig. 4. Comparison of the damping coefficient  $C_{\text{damping}}$  between experiments and simulations.

Using the definition of  $\lambda$  in (5), we can reorganize the experimental data for all lengths. The results are plotted with respect to  $\lambda$  in Fig. 4. The figure shows a clear linear relationship, which conforms to the proposed model (10).

### 2.3. Considerations for model generalization

As discussed above, the proposed linear damping model (10) is based on the experimental motivation and the dimensional analysis for cantilevers with rectangular cross-section. The aim of this work is to find a general law to describe the fluid damping for beam-type resonators with differently shaped cross-sections. To achieve this, several questions need to be considered.

- Applicability of model (10) to other types of flexural resonators.
- Determination of parameter pair  $(a, b)$  and their sensitivity to cross-section shape.
- The overall error of using model (10) for other resonators.

A numerical method to extract the fluid damping force needs to be first developed before we can attempt to generalize the fluid damping model. This is presented next.

## 3. Numerical simulation

Numerical simulation provides another way to explore the fluid damping, with the advantage of dealing with the influence of various and irregular cross-sectional shapes.

### 3.1. Simulation procedure

Finite element analysis software COMSOL is used for numerical modeling. The software provides the ability to deal with moving boundary problem using the Arbitrary–Lagrangian–Eulerian (ALE) algorithm. The procedure to find the fluid drag force contains three steps:

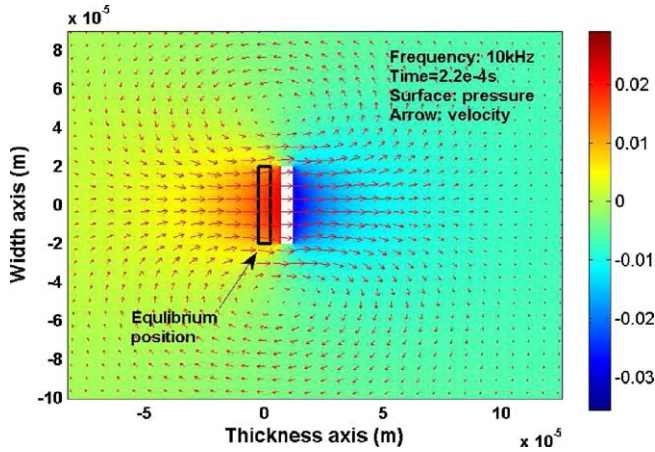


Fig. 5. COMSOL simulation of cantilever oscillation (10 kHz) in air: pressure and velocity of the fluid.

- Solve the moving boundary problem.
- Solve for the incompressible Navier–Stokes flow.
- Solve for the fluid drag force by integration around the surface.

The details of the first two steps can be referred in [12]. Fig. 5 shows the pressure and velocity distribution of the fluid (air) when a cantilever (only the rectangular cross-section is shown) is oscillating horizontally with a sinusoidal velocity. At step 3, by integrating the fluid stress and pressure around the boundary of the cross-section, the corresponding fluid drag force is also found to be sinusoidal for steady oscillation. Typical simulation results are shown in Fig. 6. Comparing the phases between the drag force and its corresponding velocity, Fig. 6 clearly shows a phase difference ( $\theta$ ). Numerically we find that this phase difference is oscillatory frequency dependent. For small frequency, the drag force is almost in-phase with the velocity ( $\theta \approx 0$ ). But for greater frequency, they can be as much as  $90^\circ$  out-of-phase ( $\theta \approx (\pi/2)$ ). In general, the drag force ( $F$ ) has two components: one is in-phase with the velocity (denoted as  $F_{\parallel}$ ) and the other is  $90^\circ$

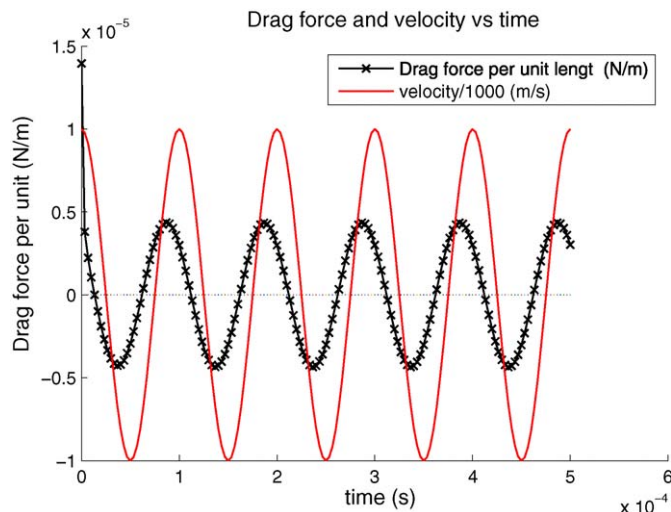


Fig. 6. Fluid drag force and the corresponding velocity: phase lag.

out-of-phase (denoted as  $F_{\perp}$ ), or

$$F_{\parallel} = F \times \cos \theta \quad (11)$$

$$F_{\perp} = F \times \sin \theta \quad (12)$$

$F_{\parallel}$  contributes to the fluid damping while  $F_{\perp}$  contributes to the additional “mass loading” to the cantilever, which will result in a resonant frequency left shift for the resonator.

### 3.2. Comparison with experiments

The simulation is carried out for different device dimensions (width and thickness for a cantilever) and different resonant frequencies. Results are plotted with respect to the parameter  $\lambda$  in Fig. 4. The comparison between the experimental data and the simulation data shows a good agreement, which not only validates the numerical analysis, but also provides a way to extract the parameter pair ( $a$ ,  $b$ ) numerically by curve fitting. For the cantilevers, from Fig. 4, we get  $a \approx 1.45$  and  $b \approx 2.06$ , or

$$C_{\text{damping}} \approx (1.45 + 2.06\lambda)\pi\mu \quad (13)$$

## 4. Model generalization

### 4.1. Parameter $b$ and its sensitivity to different cross-sections

For high resonant frequency application ( $\lambda \gg 1$ ), the parameter  $b$  will dominate the fluid damping model (10):

$$C_{\text{damping}} \approx b\lambda\pi\mu \quad (14)$$

Determination of parameter  $b$  is subjected to numerical analysis and comparison to experimental results. From the experimental and simulation results presented in Fig. 4, parameter  $b$  is extracted as:

$$b \approx 2 \quad (15)$$

Since this relation is applicable only for the rectangular cross-section with specific thickness ( $5 \mu\text{m}$  thickness for tested cantilevers), two concerns arise. The first is its sensitivity to differently shaped cross-sections. The second concern is the sensitivity of parameter  $b$  to the dimension whose direction is parallel to the flow, due to the fact that damping model (10) ignores the effect of this dimension. For the cantilever in our example, this dimension is the thickness ( $d_1$ ) in Fig. 7.

The damping coefficients for three different cross-section shapes are compared: rectangular ( $5 \mu\text{m}$  thickness,  $100 \mu\text{m}$  width), trapezoid and circular cross-sections. The results are shown in Fig. 8, from which it can be shown that the relative differences among are less than 5%. This indicates that parameter  $b$  is insensitive to device cross-section variation which could come from the design or the fabrication. But for cross-sections with non-streamlined boundary (such as the rectangle), the effect of the thickness cannot be ignored when it is comparable to the width. Numerically we compare the damping coefficients for different frequency-width combinations ( $\lambda$ ) with varying thickness. The results are shown in Fig. 9, from which it can be

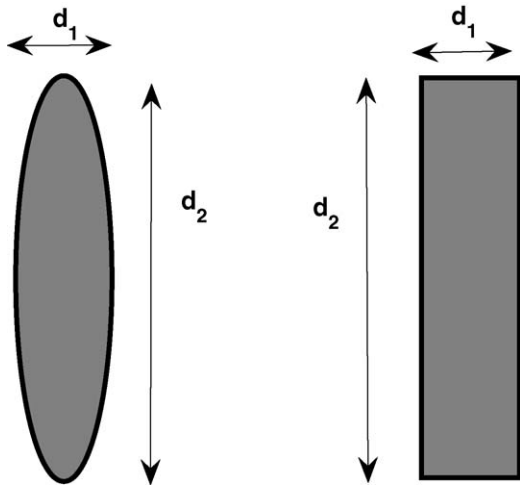


Fig. 7. Elliptical and rectangular cross-sections.

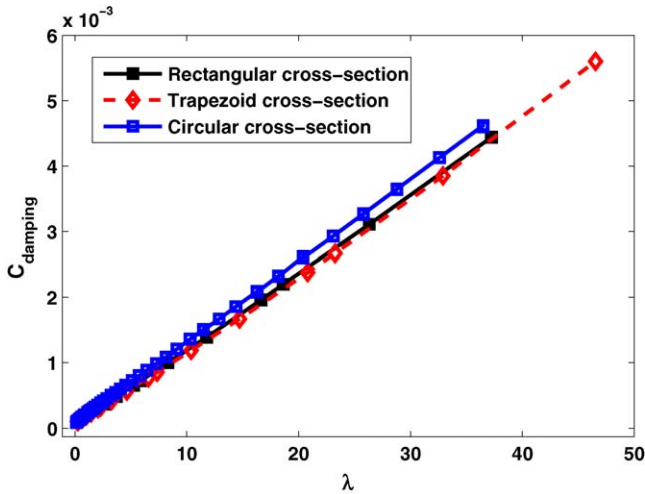


Fig. 8.  $C_{damping}$  for three types of cross-sections.

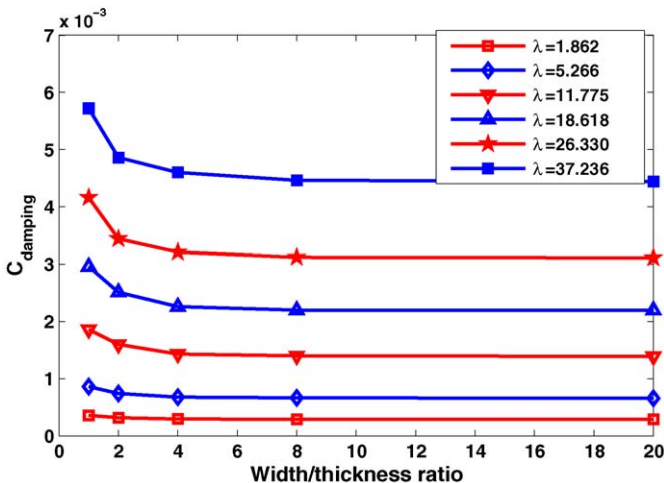


Fig. 9. Effect of the thickness on the fluid damping.

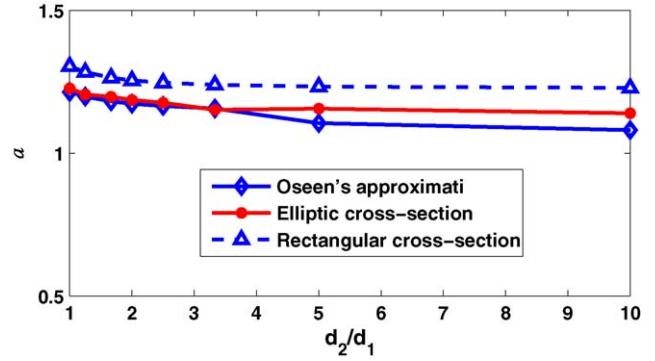


Fig. 10. Static damping: Oseen's approximation, numerical simulations.

concluded that for high width-to-thickness ratio ( $d_2/d_1 > 5$ ), the effect of the thickness is insignificant.

#### 4.2. Parameter $a$ and its sensitivity to different cross-sections

The parameter  $a$  has a dominant damping influence in (10) for systems with low frequency ( $\lambda \sim 0$ ). For the rectangular cross-section resonators such as cantilevers, there is no simple analytical expression. However, for elliptic cylinder shown in Fig. 7, Oseen [11] derived an expression for the fluid drag force, from which the corresponding  $a$  has the following form:

$$a = \frac{4}{(d_1/(d_1 + d_2)) - \gamma - \log((Re/16)((d_1 + d_2)/d_2))} \quad (16)$$

where  $\gamma$  is the Euler constant and  $Re$  is the Reynolds number. Two assumptions are made for (16). First is that the minor axis is parallel to the velocity direction ( $d_1 \parallel u$ ), the other is small Reynolds number ( $Re < 1$ ) which is usually satisfied in micro/nano fluidics. For circular cross-sections,

$$a = \frac{4}{0.5 - \gamma - \log(Re/8)} \quad (17)$$

and for cross-section with high aspect ratio ( $d_2 \gg d_1$ ),

$$a = \frac{4}{-\gamma - \log(Re/16)} \quad (18)$$

For rectangular cross-sections with high aspect ratio (shown in Fig. 7), (16) can be used as an approximation. Numerically we compare the difference of parameter  $a$  between rectangular and elliptic cross-sections, for different aspect ratio  $d_2/d_1$ . The results are plotted in Fig. 10, from which it can be concluded that approximation (16) can be safely used to model the rectangular cross-section cases with less than 10% relative error, even when  $d_2/d_1 \approx 1$ .

All the expressions for parameter  $a$  (16)–(18) are for steady flow. For oscillatory cases, because Reynolds number ( $Re$ ) is no longer uniform for the whole device, one must interpolate an average value of  $a$  according to the Reynolds number range. Fig. 11 shows the plot for expression (18).

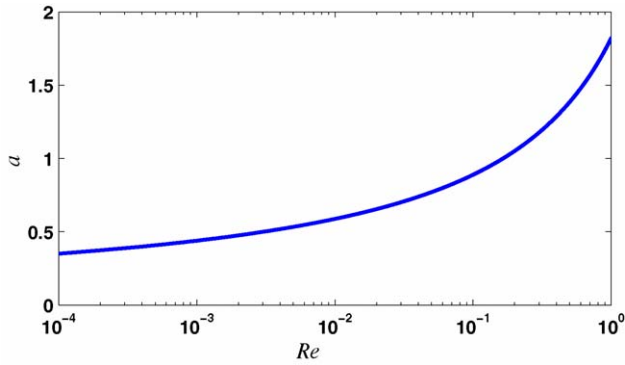


Fig. 11. Reynolds number dependent parameter  $a$ .

## 5. Discussion

In the previous section, we generalized the experimentally motivated fluid damping model to resonators with differently shaped cross-sections. Especially for high frequency applications ( $\lambda \gg 1$ ), the fluid damping model can be simplified as:

$$C_{\text{damping}} = 2\lambda\pi\mu \quad (19)$$

Expression (19) is applicable to the resonator whose cross-section has a smooth surface, such as cylinder or elliptic cylinder. For resonator with an irregular cross-section shape, high aspect ratio (at least  $>5$ ) is required for using (19) with a limited error ( $<5\%$ ).

According to (19), there are two potential applications for simple beam-type resonators: viscosity sensor and air pressure sensor. From (19), we can easily get:

$$C_{\text{damping}} = \text{width} \pi \sqrt{2\rho\omega\mu} \quad (20)$$

Also for air, the relationship between the pressure and the density is:

$$p \propto \rho \quad (21)$$

from which we can easily get:

$$C_{\text{damping}} \propto \sqrt{p} \quad (22)$$

with the assumption that the viscosity does not change with the pressure. By detecting the damping characteristics of a simple beam resonator (for example,  $Q$  factor), according to (20) and (22), we should be able to measure the fluid viscosity and the air pressure.

## 6. Conclusion

This research is aimed to improve  $Q$  factor prediction and therefore to improve the design of the flexural oscillation based micro/nano sensors and actuators which operate in high damp-

ing medium such as air or liquid. We quantitatively validate and generalize the frequency and geometry-dependent fluid damping model for micromachined flexural resonators with differently shaped cross-sections. By determining the parameter pair ( $a$ ,  $b$ ) in (10) and investigating their sensitivities to both the cross-section shape and dimension parallel to the flow, a widely applicable damping law is given in (10) and (19) with limited overall error ( $<5\%$ ) for high frequency application ( $\lambda \gg 1$ ). Although only three types of cross-section are considered in this paper, the sample represents a large constituent of technically relevant flexural oscillators.

## References

- [1] G. Stemme, Resonant silicon sensors, *J. Micromech. Microeng.* 1 (2) (1991) 113–125.
- [2] P. Enoksson, G. Stemme, E. Stemme, Fluid density sensor based on resonance vibration, *Sens. Actuator A* 47 (1995) 327–331.
- [3] K.Y. Yasummura, T.D. Stowe, E.M. Chow, T. Pfafman, T.W. Kenny, B.C. Stipe, D. Rugar, Quality factors in micron and submicron thick cantilevers, *J. MEMS* 9 (1) (2000) 117–125.
- [4] M.K. Ghatkesar, Real-time mass sensing by nanomechanical resonators in fluid, *IEEE Sens. Vienna* (2004).
- [5] W. Zhang, K.L. Turner, Application of parametric resonance amplification in a single-crystal silicon micro-oscillator based mass sensor, *Sens. Actuators A: Phys.* V122 (2005) 23–30.
- [6] K. Aihara, J. Xiang, S. Chopra, A. Pham, R. Apprao, GHz Carbon Nanotube Resonator Biosensors, *IEEE Nanotechnologies*, San Francisco, USA, 2003.
- [7] W.E. Newell, Miniaturization of tuning forks, *Science* 161 (1968) P1320–P1326.
- [8] F.R. Blom, S. Bouwstra, M. Elwenspoek, J.H.J. Fluitman, Dependence of the  $Q$  factor of micro-machined silicon beam resonators on pressure and geometry, *J. Vac. Sci. Technol. B* 10 (1) (1992) 19–26.
- [9] L.D. Landau, E.M. Lifshitz, *Fluid Mechanics*, Pergamon Press, London, 1959.
- [10] TurnerF K.L., et al., Five parametric resonances in a microelectromechanical system, *Nature* 396 (1998) 149–152.
- [11] H. Lamb, *Hydrodynamics*, Dover Publications, New York, 1945.
- [12] COMSOL manual and demo, <http://www.comsol.com/showroom/>.

## Biographies

**Weibin Zhang** received his BS (1996) and MS (1999) in Mechanical Engineering Department from Peking University. Currently he is a PhD candidate in University of California, Santa Barbara. His research interests include dynamics of micro/nano systems, sensor development and control, micro/nano devices modeling, testing and characterization.

**Kimberly Turner** received her BS in mechanical engineering from Michigan Technological University in 1994 and her PhD in theoretical and applied mechanics from Cornell University in 1999. She is currently an Associate Professor of Mechanical and Environmental Engineering at the University of California, Santa Barbara. Dr. Turners research interests include nonlinear dynamics of micro/nanoscale systems, testing and characterization of MEMS devices, modeling of micro/nanoscale devices, and solid-state sensor development.